Electronic Supplementary Material (ESI) for Journal of Materials Chemistry A.

Benzocyclobutene Polymer as an Additive for a Benzocyclobutene-Fullerene: Application in Stable p-i-n Perovskite Solar Cells

Marie-Hélène Tremblay[a], Kelly Schutt[b], Federico Pulvirenti[a], Thorsten Schultz[c, d], Berthold Wegner[c, d], Xiaojia Jia[e], Yadong Zhang[a], Elena Longhi[a], Raghunath R. Dasari[a], Canek Fuentes Hernandez[e], Bernard Kippelen[e], Norbert Koch[c, d], Henry J. Snaith[b], Stephen Barlow[a], Seth R. Marder[a]*

[a] School of Chemistry and Biochemistry, and Center for Organic Photonics and Electronics (COPE), Georgia Institute of Technology, Atlanta, GA, 30332, United States

[b] Clarendon Laboratory, Department of Physics, University of Oxford, Oxford, OX1 3PU, United Kingdom

[c] Humboldt-Universität zu Berlin, Institut für Physik & IRIS Adlershof, Berlin, 12489, Germany

[d] Helmholtz-Zentrum für Materialien und Energie GmbH, Berlin, 12489, Germany

[e] School of Electrical and Computer Engineering, and Center for Organic Photonics and Electronics (COPE), Georgia Institute of Technology, Atlanta, GA, 30332, United States

*Corresponding author: Seth R. Marder, seth.marder@chemistry.gatech.edu

Contents

1 Experimental

Materials Synthesis

PCBCB and $(IrCp^*Cp)_2$ were synthesized as reported previously.[1, 2] Bicyclo[4.2.0]octa-1,3,5-trien-7-ol, **1**, was synthesized in two steps as reported previously.[3]

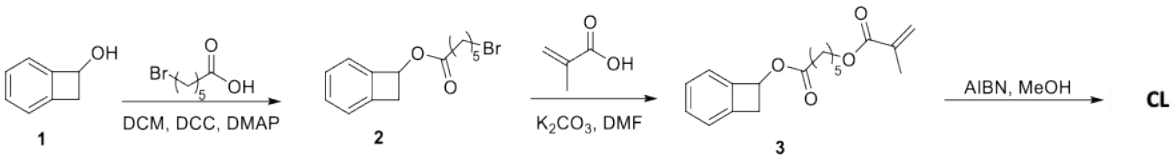

Bicyclo[4.2.0]octa-1(6),2,4-trien-7-yl 6-bromohexanoate (**2**). To a solution of bicyclo[4.2.0]octa-1,3,5-trien-7-ol (0.65 g, 5.4 mmol) and 6-bromohexanoic acid (1.11 g, 5.7 mmol) in dry dichloromethane (20.0 mL) were added *N,N′*-dicyclohexylcarbodiimide (1.23 g, 6 mmol) and 4-dimethylaminopyridine (0.05 g, 0.4 mmol) at room temperature under stirring. The reaction was carried out at room temperature for 2 h. The reaction mixture was filtered, and the solvent was removed. A yellow oil was obtained (2.45 g, 91%) after column chromatography using $CHCl_3$ and ethanol (100:1) as eluent. ^{1}H NMR (300 MHz, $CDCl_3$): δ 7.32 (m, 2H), 7.24 (m, 1H), 7.15 (d, $J_{H\text{-}H}$ = 6 Hz, 1H), 5.92 (dd, $J_{H\text{-}H}$ = 3.0, 1.5 Hz, 1H), 3.66 (dd, $J_{H\text{-}H}$ = 15.0 Hz, 3.0 Hz, 1H), 3.40 (t, $J_{H\text{-}H}$ = 6.0 Hz, 2H), 3.22 (dd, $J_{H\text{-}H}$ = 15.0 Hz, 1.5 Hz, 1H), 2.38 (t, $J_{H\text{-}H}$ = 6 Hz, 2H), 1.88 (p, $J_{H\text{-}H}$ = 9.0 Hz, 2H), 1.69 (p, $J_{H\text{-}H}$ = 6.0 Hz, 2H), 1.49 (m, 2H). ^{13}C{^{1}H} NMR (100.62 MHz, dimethyl sulfoxide-d_6): δ 172.88, 144.05, 142.51, 130.00, 127.52, 123.33, 123.30, 71.02, 38.55, 34.97, 33.19, 31.86, 26.99, 23.55. Anal. Calcd. for $C_{14}H_{17}BrO_2$: C, 56.58; H 5.77; found: C, 56.44; H, 5.68. MS (ESI) *m/z* 319.03 [$C_{14}H_{17}O_2BrNa$ $(M+Na)^+$].

Bicyclo[4.2.0]octa-1(6),2,4-trien-7-yl 6-(methacryloyloxy)hexanoate (**3**). To a solution of methacrylic acid (1.05 g, 12.2 mmol) in dry DMF (10.0 mL) at room temperature, potassium carbonate (1.03 g, 18.3 mmol) and a solution of bicyclo[4.2.0]octa-1(6),2,4-trien-7-yl 6-bromohexanoate (0.9 g, 3.1 mmol) in DMF (2.0 mL) were added under nitrogen. Light exposure of the reaction was minimized by wrapping the flask in aluminum foil. The reaction was monitored by thin layer chromatography. After 72 h the reaction was halted, the product was extracted in ether, and the extracts were washed with water at least three times. The organic residue was dried on Na_2SO_4, and the solvent was removed. A column was performed using a Biotage flash purification system (70% hexanes : 30% ethyl acetate) without exposing the crude material to light or heating. The organic phase was collected and the product extracted in water. The solvent was removed under reduced pressure. The product (0.46 g, 50% yield) and the starting material (250 mg, 0.86 mmol) bicyclo[4.2.0]octa-1(6),2,4-trien-7-yl 6-bromohexanoate were isolated. ^{1}H NMR (500 MHz, $CDCl_3$): δ 7.32 (td, $J_{H\text{-}H}$ = 6.0, 0.5 Hz, 1H), 7.24 (m, 2H), 7.15 (d, $J_{H\text{-}H}$ = 6.0 Hz, 1H), 6.09 (m, 1H), 5.92 (dd, $J_{H\text{-}H}$ = 3.0, 1.5 Hz, 1H), 5.54 (m, 1H), 4.14 (t, $J_{H\text{-}H}$ = 6.0 Hz, 2H), 3.66 (dd, $J_{H\text{-}H}$ = 15.0 Hz, 3.0 Hz, 1H), 3.21 (d, $J_{H\text{-}H}$ = 15.0 Hz, 1H), 2.38 (t, $J_{H\text{-}H}$ = 6 Hz, 2H), 1.93 (s, 3H), 1.71 (m, 4H), 1.44 (m, 2H). ^{13}C(^{1}H) NMR (125.81 MHz, $CDCl_3$): δ 173.54, 167.48, 144.26, 142.72, 136.45, 129.98, 127.54, 125.28,

123.53, 123.22, 71.51, 64.46, 38.95, 34.09, 28.33, 25.61, 24.56, 18.34. Anal. Calcd. for $C_{18}H_{22}O_4$: C, 71.50; H 7.33; found: C, 71.46; H, 7.51. MS (ESI) *m/z* 303.15 [$C_{18}H_{23}O_4$ $(M+H)^+$].

Poly(bicyclo[4.2.0]octa-1(6),2,4-trien-7-yl 6-(methacryloyloxy)hexanoate) (**CL**). **3** (0.40 g, 1.32 mmol) and AIBN (2.0 mg, 0.012 mmol) were dissolved in dry benzene (6 ml) under nitrogen. The polymerization mixture was deoxygenated and was then heated up at 60 °C for 7 days without light exposure. The polymer was precipitated into methanol three times. After drying under vacuum, a white polymer was obtained (0.32 g, 80%). ^{1}H NMR (500 MHz, $CDCl_3$): δ 7.28 (m, 1H), 7.20 (m, 2H), 7.11 (d, $J_{H\text{-}H}$ = 10 Hz, 1H), 5.87 (s, 1H), 3.89 (s, br, 2H), 3.61 (dd, $J_{H\text{-}H}$ = 15.0 Hz, 5.0 Hz, 1H), 3.17 (d, $J_{H\text{-}H}$ = 15.0 Hz, 1H), 2.34 (s, br, 2H), 1.77 (m, br, 2H), 1.65 (m, br, 2H), 1.58 (s, 3H), 1.36 (s, br, 2H), 0.99 (s, br, 2H). ^{13}C{^{1}H} NMR (125.81 MHz, $CDCl_3$): δ 177.45, 173.54, 144.43, 142.81, 130.07, 127.65, 123.69, 123.33, 71.60, 64.87, 54.24, 45.02, 39.05, 34.08, 27.99, 25.70, 24.62, 16.86. Anal. Calcd. for $C_{18}H_{22}O_4$: C, 71.50; H 7.33; found: C, 71.41; H, 7.36. [$C_{18}H_{22}O_4$]. M_w = 580 kDa, M_n = 290 kDa, Đ = 2 (determined via GPC in $CHCl_3$ at 35 °C). T_g = -10 °C, T_d = 210 °C.

Characterization techniques

Nuclear Magnetic Resonance (NMR). NMR spectra were acquired using a Bruker Avance III 500 MHz spectrometer using $CDCl_3$ as the solvent at 25 °C. The chemical shifts were calibrated using the residual proton signal or the ^{13}C signal of the solvent as an internal reference ($CDCl_3$: 7.26 ppm for ^{1}H NMR, 77.00 ppm for ^{13}C NMR).

Gel Permeation Chromatography (GPC). GPC was performed using a Tosoh EcoSEC HT GPC instrument with RI detector. Experiments were run with chloroform as eluent at 140 °C at a flow rate of 1 mL min^{-1} on two sequentially connected 30 × 7.8 mm GMHhr-H(S) HT2 columns (Tosoh Bioscience). The instrument was calibrated vs. polystyrene standards (1,390−1,214,000 g/mol), and data were analyzed using EcoSEC High Temperature GPC Workstation Software. To prepare polymer sample for GPC measurement, the polymer was dissolved in HPLC grade chloroform at a concentration of 1.0 mg mL^{-1} and then stirred overnight prior to filtering through a 0.45 mm PTFE filter.

Thermogravimetric Analyses (TGA). TGA were measured under nitrogen atmosphere on a Pyris 1 TGA (PerkinElmer) at a heating rate of 15 °C/min from 50-700 °C.

X-ray Photoelectron Spectroscopy (XPS). XPS measurements for the washing experiments were performed at a JEOL JPS-9030 setup, using monochromatic Al Kα radiation for excitation and a pass energy of 30 eV. The samples were transferred from a glovebox to the UHV system without exposure to air.

Ultraviolet Photoelectron Spectroscopy (UPS). UPS measurements were performed using a helium discharge lamp for excitation. Aluminum filters were used to reduce the photon flux and the exposure time was kept to a minimum to minimize charging of the samples. A bias of 10 V was applied for the secondary electron cut-off measurements.

UV-vis-NIR Absorption Spectroscopy. Absorbance spectra were measured with a Lambda 1050 UV-vis-NIR spectrophotometer (PerkinElmer) in a controlled nitrogen atmosphere. The solutions were prepared and sealed in the cuvettes in a glovebox. A baseline spectrum of dichlorobenzene was subtracted from the spectra before further analysis.

Steady-State Photoluminescence. Steady state photoluminescence was measured using a Horiba Fluorolog-3 with an InGaAs detector.

Time-Resolved Photoluminescence. Time resolved photoluminescence was measured using a time correlated single photon counting (TCSPC) setup (FluoTime 300 PicoQuant GmbH). Samples were photoexcited with a 507 nm laser head (LDH-P-C-510, PicoQuant GmbH) at frequencies between 0.5 and 2 MHz with a pulse duration of 117 ps and a detection wavelength of 775 nm.

PL Data Treatment. Each normalized PL decay was fitted to a stretched exponential function following the method of Stranks *et al*.:[4]

$$I(t) = exp\left[-\left(\frac{t - t_0}{\tau}\right)^{\beta}\right]$$

with I(t) the PL intensity at time t, t_0 an offset correction (constrained such that $0 \leq t_0 \leq 10$), τ the characteristic lifetime and β the stretching exponent. The use of a stretched exponential function to fit PL data from perovskite films is well established in the literature, in lieu of a true analytical model.[5, 6] The stretching of the exponential has been interpreted as resulting from a distribution of monomolecular (trap-assisted) non-radiative decay rates within the material.[7] The mean relaxation time, $\langle\tau\rangle$, given by Equation 4:

$$\langle\tau\rangle = \frac{\tau}{\beta}\Gamma\left(\frac{1}{\beta}\right)$$

where Γ(z) is the gamma function:

$$\Gamma(z) = \int_0^{\infty} x^{z-1}e^{-x}dx$$

Transmission Line Measurements. All films of the electron transporting materials [i.e., PCBM and $(PCBCB)_n$, with and without addition of dopant or crosslinker] had a thickness of 50 nm, measured via ellipsometry. To keep the thickness of the ETM constant, the final concentration of all fullerene solutions, with and without the addition of *n*-dopant and/or crosslinker, was set to 30 mg mL^{-1}. For doping concentrations > 1 mol%, the concentration of $(IrCp^*Cp)_2$ and PCBCB solutions was fixed to 17 mg mL^{-1} in chlorobenzene and 50 mg/mL in dichlorobenzene, respectively; for doping concentrations < 1 mol%, the concentration of $(IrCp^*Cp)_2$ and PCBCB solutions was fixed to 2 mg/mL in chlorobenzene and 31 mg/mL in dichlorobenzene, respectively. 5 mg of crosslinker were

dissolved in 1 mL of dichlorobenzene. All solutions were prepared, stirred for at least 6 h, and spin-coated at 2000 rpm, 2000 rpm s^{-1}, for 45 s onto detergent/solvent-cleaned glass substrates in a glovebox (<0.5 ppm water and <50 ppm oxygen), using degassed and anhydrous solvents. PCBM films – obtained from 30 mg mL^{-1} solutions in chlorobenzene – were annealed at 70 °C for 10 min, while PCBCB-based films were annealed at 200 °C for 10 min to effect insolubilization. All films were immediately transferred without air exposure to a vacuum thermal evaporation system (SPECTROS, K. J. Lesker), for the deposition of silver metal (100 nm).

Current−Voltage (JV) Measurements. The *JV* curves were measured (2400 Series SourceMeter, Keithley Instruments) under simulated AM 1.5 sunlight at 100 mW cm^{-2} irradiance generated by an Abet Class AAB sun 2000 simulator, with the intensity calibrated with an NREL calibrated KG 5 filtered Si reference cell. The forward *J–V* scans were measured from forward bias to short circuit and the backward scans were from short circuit to forward bias, both at a scan rate of 380 mV s^{-1}. A stabilization time of 5 s at forward bias of 0 V under illumination was employed prior to scanning.

Device preparation

Substrate Preparation. Fluorine-doped tin oxide (FTO) coated glass substrates (Pilkington TEC 7) were used here. FTO was etched at specific regions using a 2M HCl and zinc powder. Substrates were then cleaned with water, then sequentially sonicated for 5 minutes in water, acetone and isopropyl alcohol, and dried with a compressed nitrogen gun. Next, the substrates were treated for 15 min with UV ozone.

F_4TCNQ-Doped PolyTPD. 0.2 mg of F_4TCNQ (Dyesol) and 1 mg of PolyTPD were added to 1 mL of toluene. The solution was stirred for 12 h prior to deposition. The filtered solution was spincoated at 2000 rpm, 2000 rpm s^{-1} for 20 s and dried at 130 °C for 10 min.

$Cs_{0.05}(FA_{0.85}MA_{0.15})_{0.95}Pb(I_{0.9}Br_{0.1})_3$ Perovskite (FAMACs). The precursor solution was prepared by dissolving formamidinium iodide (FAI; Dyesol), methylammonium iodide (MAI; Dyesol), cesium iodide (CsI; Sigma Aldrich), lead iodide (PbI_2; TCI) and lead bromide ($PbBr_2$; Alfa Aesar) in anhydrous *N,N*-dimethylformamide (DMF; Sigma-Aldrich) and dimethylsulfoxide (DMSO; Sigma-Aldrich) in a ratio 4:1 in a nitrogen-filled glovebox to obtain a stoichiometric 1.3 M solution. The solution was then stirred overnight at room temperature and filtered using a 0.44 μm filter. 150 μL of the precursor perovskite solution was spin-coated in a drybox at 1000 rpm for 10 s and then 6000 rpm for 35 s with a ramp of 2000 rpm s^{-1}. After 35 s, 400 μL of toluene (Sigma) was quickly added on the spinning substrates. The films were dried on a hot plate at a temperature of 100 °C for 60 min.

Electron-Transport Material. PCBM (PCBM = phenyl-C_{61}-butyric acid methyl ester) (20 mg mL^{-1} in 3:1 chlorobenzene/dichlorobenzene) was stirred overnight prior to deposition.

PCBM was deposited by spin coating at 2000 rpm for 20 s, followed by annealing for 5 min at 100 °C.

PCBCB (30 mg mL^{-1} in dichlorobenzene), $(IrCp^*Cp)_2$ (2.4 mg mL^{-1} in chlorobenzene) and CL (12 mg mL^{-1} in dichlorobenzene) were dissolved and stir overnight prior to deposition. The filtered solutions were mixed with dichlorobenzene to obtain the right ratio of PCBCB:crosslinker:$(IrCp^*Cp)_2$ with a final concentration of PCBCB of 20 mg mL^{-1}. The prepared solutions were spin coated at 2000 rpm, 2000 rpm s^{-1} for 20 s and crosslinked on a hotplate at 150 °C for 5 min in a N_2-filled glovebox.

BCP (BCP = bathocuproine) (0.5 mg mL^{-1} in isopropanol) was stirred overnight prior to deposition. BCP was deposited by spin coating at 5000 rpm for 20 s followed by annealing at 100 °C for 1 min.

Electrode Evaporation. An 100 nm silver or 80 nm gold electrode was thermally evaporated under vacuum.

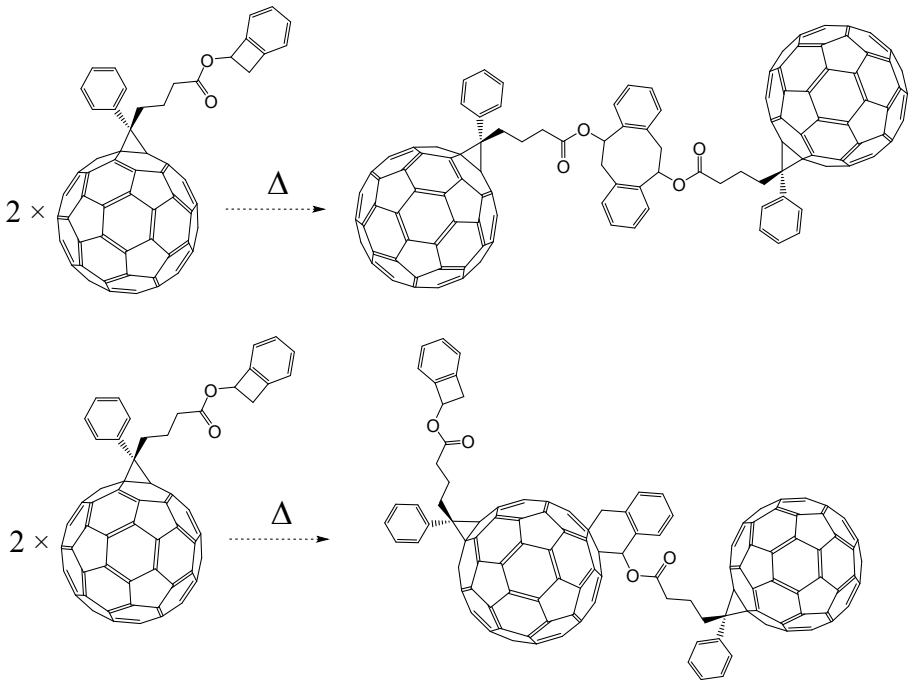

Figure S1. Thermally activated reactions of PCBCB molecules, where two benzocyclobutene groups can react together (top), and where a benzocyclobutene group reacts with the fullerene cage (bottom).

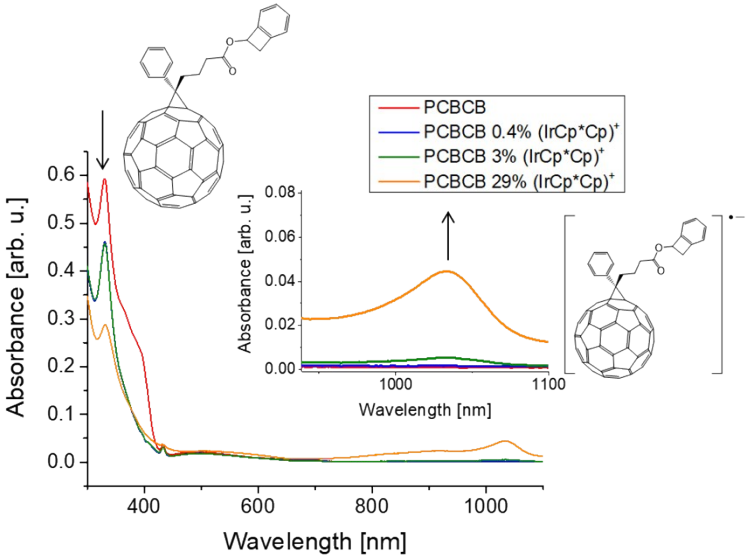

Figure S2. UV-vis-NIR absorption spectra of solutions of PCBCB in chlorobenzene as a function of $(IrCp^*Cp)^+$ content (molar percentage). The inset shows the appearance of the PCBCB radical anion at 1070 nm and the disappearance of neutral PCBCB at 330 nm.

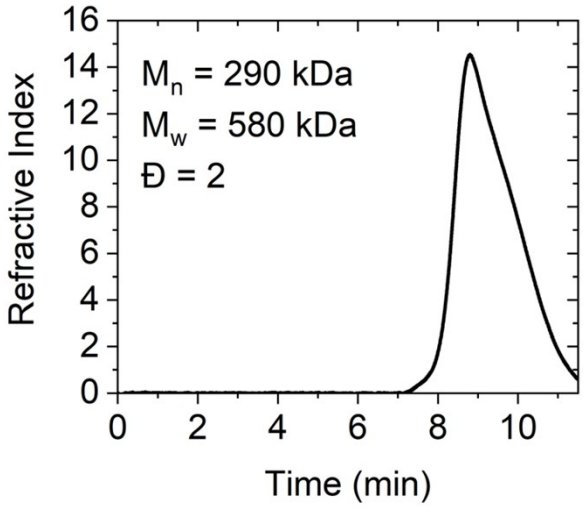

Figure S3. Gel permeation chromatography of $(PCBCB)_n$ solution using chloroform as eluent at 140 °C at a flow rate of 1 mL min^{-1}.

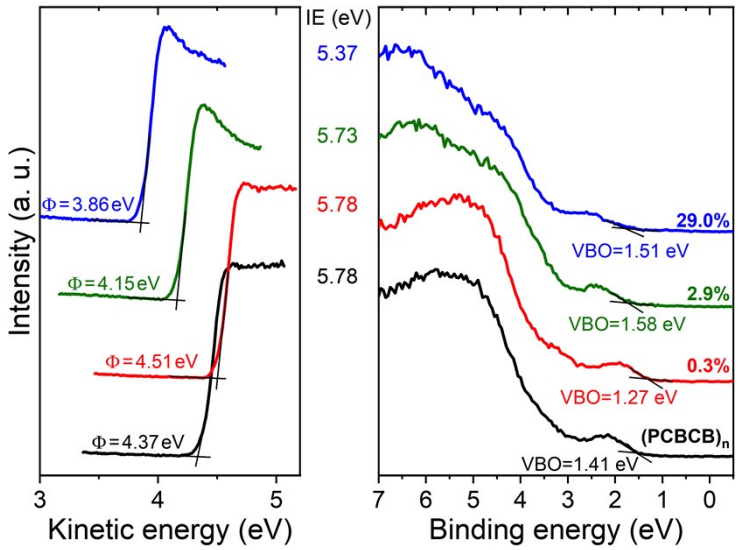

Figure S4. UPS spectra of neat and doped $(PCBCB)_n$ film with $(IrCp^*Cp)_2$. Dimer content is reported as a function of nominal molar percentage of monomer cations $(IrCp^*Cp)^+$ relative to the host.

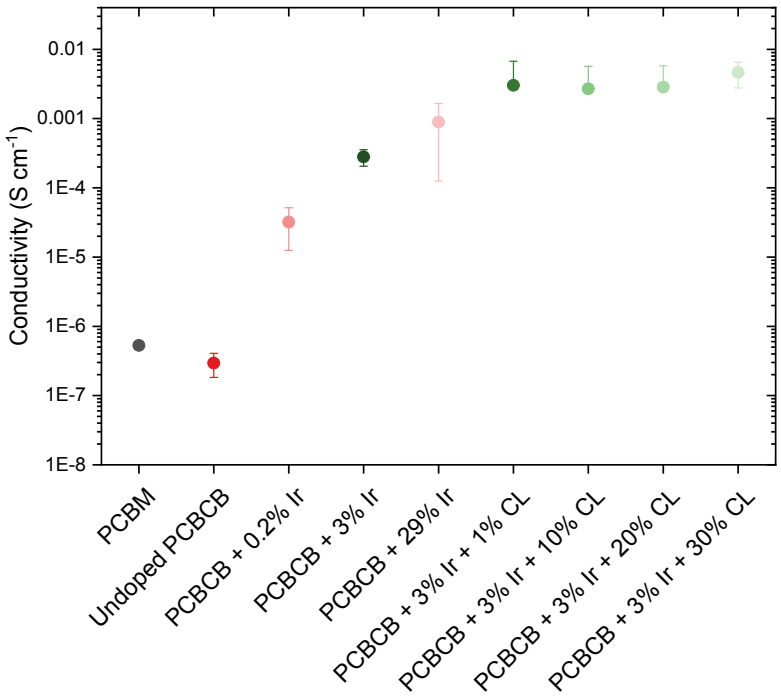

Figure S5. Conductivity of $(PCBCB)_n$ with silver electrodes as a function of nominal $(IrCp^*Cp)^+$ content (molar percentage) and CL content. The conductivity of PCBM is reported for comparison.

Table S1. Sheet resistance of $(PCBCB)_n$, resistance at the $(PCBCB)_n$/silver contact and conductivity of $(PCBCB)_n$ as a function of $(IrCp^*Cp)^+$ content (molar percentage). The resistivity and conductivity of PCBM are reported for comparison.

Material	R_s (Ω □$^{-1}$)	R_c (Ω)	σ (S cm^{-1})
PCBM	$2.8 \times 10^{12} \pm 4.4 \times 10^{12}$	$8.2 \times 10^{10} \pm 6.9 \times 10^{10}$	$5.6 \times 10^{-7} \pm 5.0 \times 10^{-7}$
$(PCBCB)_n$	$6.7 \times 10^{11} \pm 3.1 \times 10^{11}$	$5.4 \times 10^{9} \pm 3.8 \times 10^{9}$	$3.7 \times 10^{-7} \pm 2.2 \times 10^{-7}$
$(PCBCB)_n$ 0.2% $(IrCp^*Cp)^+$	$5.3 \times 10^{9} \pm 2.9 \times 10^{9}$	$2.9 \times 10^{7} \pm 2.4 \times 10^{7}$	$4.5 \times 10^{-5} \pm 1.9 \times 10^{-5}$
$(PCBCB)_n$ 3% $(IrCp^*Cp)^+$	$1.0 \times 10^{9} \pm 9.4 \times 10^{8}$	$1.6 \times 10^{7} \pm 1.3 \times 10^{7}$	$3.3 \times 10^{-4} \pm 2.3 \times 10^{-4}$
$(PCBCB)_n$ 29% $(IrCp^*Cp)^+$	$1.5 \times 10^{8} \pm 3.7 \times 10^{7}$	$1.4 \times 10^{6} \pm 1.0 \times 10^{6}$	$1.4 \times 10^{-3} \pm 3.8 \times 10^{-4}$

Table S2. Sheet resistance of doped $(PCBCB)_n$, resistance at the doped $(PCBCB)_n$/silver contact and conductivity as a function of crosslinker concentration. The $(IrCp^*Cp)^+$ concentration was fixed to 3 mol%.

Material	R_s (Ω □$^{-1}$)	R_c (Ω)	σ (S cm^{-1})
PCBM	$2.8 \times 10^{12} \pm 4.4 \times 10^{12}$	$8.2 \times 10^{10} \pm 6.9 \times 10^{10}$	$5.6 \times 10^{-7} \pm 5.0 \times 10^{-7}$
$(PCBCB)_n$ 3% $(IrCp^*Cp)^+$	$1.0 \times 10^{9} \pm 9.4 \times 10^{8}$	$1.6 \times 10^{7} \pm 1.3 \times 10^{7}$	$3.3 \times 10^{-4} \pm 2.3 \times 10^{-4}$
$(PCBCB)_n$ 3% $(IrCp^*Cp)^+$ 1% crosslinker	$3.7 \times 10^{7} \pm 3.6 \times 10^{6}$	$9.6 \times 10^{5} \pm 4.9 \times 10^{5}$	$5.5 \times 10^{-3} \pm 5.4 \times 10^{-4}$
$(PCBCB)_n$ 3% $(IrCp^*Cp)^+$ 10% crosslinker	$4.3 \times 10^{7} \pm 5.8 \times 10^{6}$	$7.7 \times 10^{5} \pm 1.8 \times 10^{5}$	$4.7 \times 10^{-3} \pm 6.8 \times 10^{-4}$
$(PCBCB)_n$ 3% $(IrCp^*Cp)^+$ 20% crosslinker	$4.3 \times 10^{7} \pm 7.1 \times 10^{6}$	$2.8 \times 10^{5} \pm 2.2 \times 10^{5}$	$4.8 \times 10^{-3} \pm 8.8 \times 10^{-4}$
$(PCBCB)_n$ 3% $(IrCp^*Cp)^+$ 30% crosslinker	$4.4 \times 10^{7} \pm 2.9 \times 10^{7}$	$2.7 \times 10^{6} \pm 6.4 \times 10^{5}$	$5.9 \times 10^{-3} \pm 3.4 \times 10^{-3}$

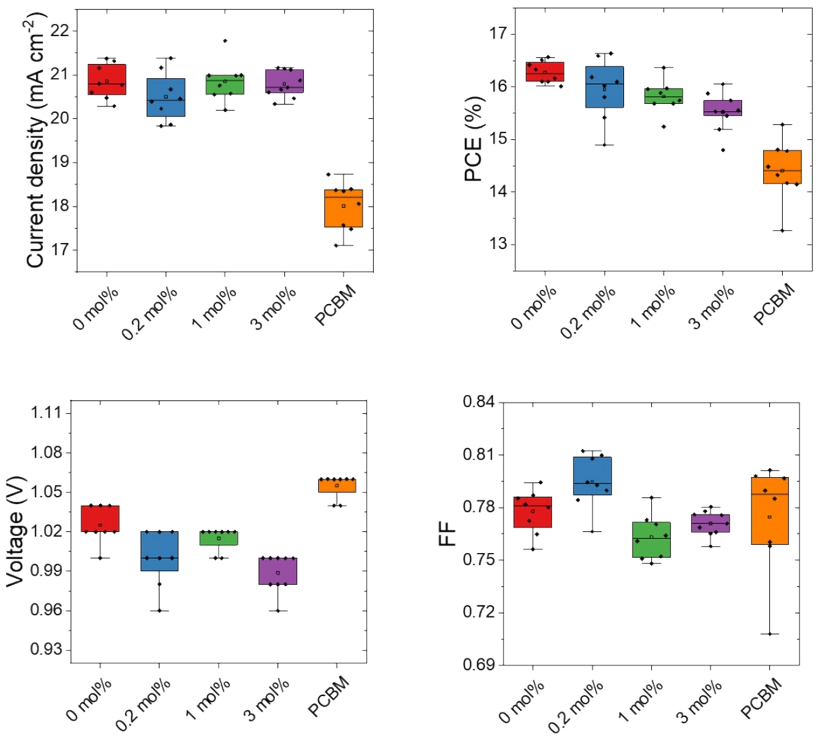

Figure S6 Comparing the photovoltaic performance of FAMACs devices with $(PCBCB)_n$·CL at different concentration of $(IrCp^*Cp)_2$. Box-plot of devices prepared in 1 batch showing the comparison of the PV parameters (from J-V curves) of devices made using $(PCBCB)_n$·CL and PCBM.

Table S3 Statistics for FAMACs devices made to optimize the concentration of dopant used to cast **$(PCBCB)_n$·CL** films (concentration **P1-2:** 20 mg mL^{-1}, concentration of **CL:** 20 mol%).

		J_{sc} (mA cm^{-2})	V_{OC} (V)	FF	PCE (%)
$(PCBCB)_n$·CL	**Average**	20.8 ± 0.4	1.03 ± 0.01	0.78 ± 0.01	16.3 ± 0.2
	Maximum	21.38	1.04	0.79	16.56
$(PCBCB)_n$·CL with $(IrCp^*Cp)_2$ (0.2 mol%)	**Average**	20.5 ± 0.6	1.00 ± 0.02	0.79 ± 0.01	16.0 ± 0.6
	Maximum	21.38	1.02	0.81	16.63
$(PCBCB)_n$·CL with $(IrCp^*Cp)_2$ (1 mol%)	**Average**	20.9 ± 0.5	1.02 ± 0.01	0.76 ± 0.01	15.8 ± 0.3
	Maximum	21.78	1.02	0.79	16.37
$(PCBCB)_n$·CL with $(IrCp^*Cp)_2$ (3 mol%)	**Average**	21.8 ± 0.3	0.99 ± 0.01	0.77 ± 0.01	15.5 ± 0.4
	Maximum	21.16	1.00	0.78	16.05
PCBM	**Average**	18.0 ± 0.6	1.06 ± 0.01	0.77 ± 0.03	14.4 ± 0.6
	Maximum	18.73	1.06	0.80	15.28

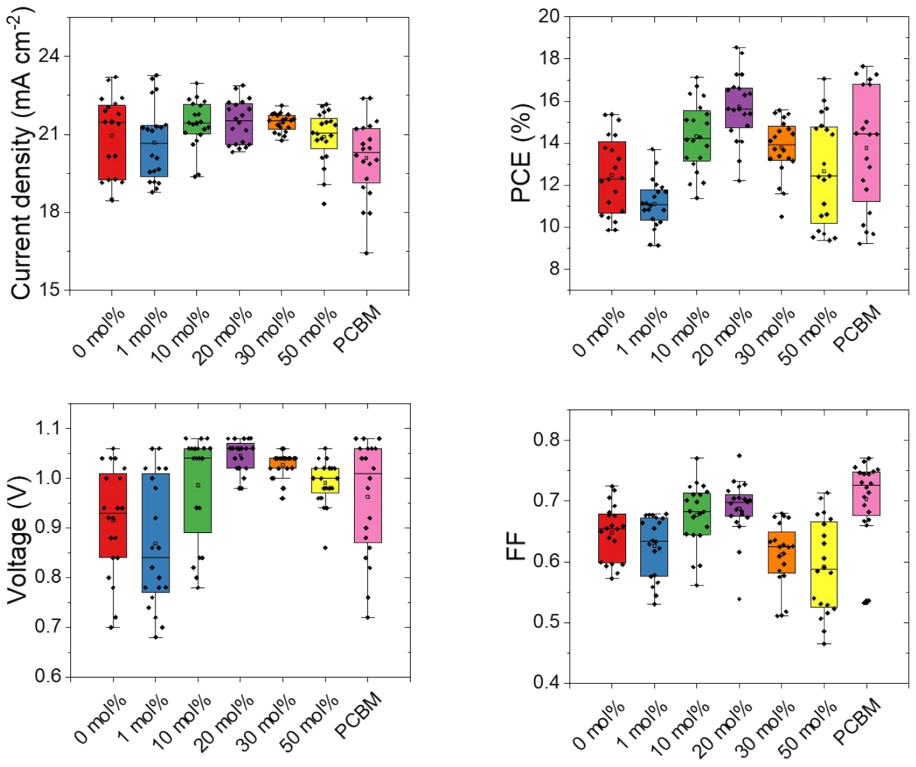

Figure S7 Comparing the photovoltaic performance of FAMACs devices with $(PCBCB)_n$·CL at different concentration of CL. Box-plot of devices prepared in 1 batch showing the comparison of the PV parameters (from J-V curves) of devices made using $(PCBCB)_n$·CL and PCBM.

Table S4 Statistics for FAMACs devices made to optimize the concentration of CL used to cast **$(PCBCB)_n$·CL** films (concentration **P1-2:** 20 mg mL^{-1}).

		J_{sc} (mA cm^{-2})	V_{OC} (V)	FF	PCE (%)
$(PCBCB)_n$	**Average**	21 ± 2	0.9 ± 0.1	0.65 ± 0.05	12 ± 2
	Maximum	23.20	1.06	0.72	15.35
$(PCBCB)_n$·CL (1 mol%)	**Average**	21 ± 1	0.9 ± 0.1	0.63 ± 0.05	11 ± 1
	Maximum	23.27	1.06	0.68	13.70
$(PCBCB)_n$·CL (10 mol%)	**Average**	21.4 ± 0.9	1.0 ± 0.1	0.67 ± 0.05	14 ± 2
	Maximum	22.96	1.08	0.77	17.12
$(PCBCB)_n$·CL (20 mol%)	**Average**	21.5 ± 0.8	1.05 ± 0.03	0.69 ± 0.05	16 ± 2
	Maximum	22.87	1.08	0.78	18.54
$(PCBCB)_n$·CL (30 mol%)	**Average**	21.4 ± 0.3	1.03 ± 0.03	0.61 ± 0.05	14 ± 1
	Maximum	22.10	1.06	0.68	15.57
$(PCBCB)_n$·CL (50mol%)	**Average**	21 ± 1	0.99 ± 0.05	0.59 ± 0.08	13 ± 3
	Maximum	22.14	1.06	0.71	17.06
PCBM	**Average**	20 ± 2	1.0 ± 0.1	0.70 ± 0.07	14 ± 3
	Maximum	22.39	1.08	0.77	17.65

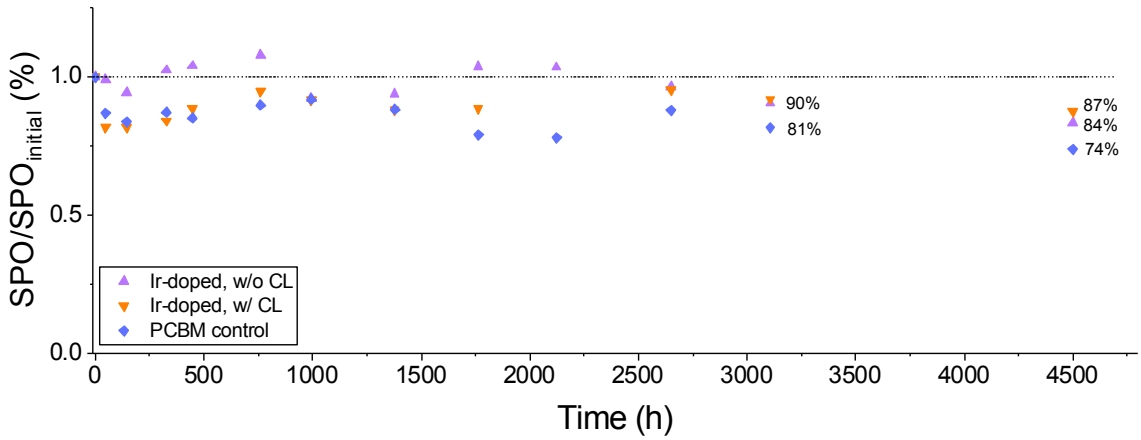

Figure S8. Stability comparison of non-encapsulated perovskite solar cells (PSCs) fabricated using doped $(PCBCB)_n$, doped $(PCBCB)_n$·CL (20 mol%) and PCBM made from the same batch. An average of four devices per each data point is reported. The SPO is normalized to the initial SPO.

References

1. K. Wojciechowski, I. Ramirez, T. Gorisse, O. Dautel, R. Dasari, N. Sakai, J. M. Hardigree, S. Song, S. Marder, M. Riede, G. Wantz and H. J. Snaith, *ACS Energy Lett.*, 2016, **1**, 648-653.
2. O. V. Gusev, M. G. Peterleitner, M. A. Ievlev, A. M. Kal'sin, P. V. Petrovskii, L. I. Denisovich and N. A. Ustynyuk, *J.Organomet. Chem.*, 1997, **531**, 95-100.
3. W. Bubb and S. Sternhell, *Aust. J. Chem.*, 1976, **29**, 1685-1697.
4. S. D. Stranks, G. E. Eperon, G. Grancini, C. Menelaou, M. J. P. Alcocer, T. Leijtens, L. M. Herz, A. Petrozza and H. J. Snaith, *Science*, 2013, **342**, 341.
5. G. E. Eperon, S. D. Stranks, C. Menelaou, M. B. Johnston, L. M. Herz and H. J. Snaith, *Energ. Environ. Sci.*, 2014, **7**, 982-988.
6. D. W. de Quilettes, S. M. Vorpahl, S. D. Stranks, H. Nagaoka, G. E. Eperon, M. E. Ziffer, H. J. Snaith and D. S. Ginger, *Science*, 2015, **348**, 683.
7. D. W. deQuilettes, S. Koch, S. Burke, R. K. Paranji, A. J. Shropshire, M. E. Ziffer and D. S. Ginger, *ACS Energy Lett.*, 2016, **1**, 438-444.